Available online at www.sciencedirect.com
SCIENCE DIRECT®
Applied Surface Science 230 (2004) 232–240
applied surface science
www.elsevier.com/locate/apsusc

Alkylsilane self-assembled monolayers: modeling their wetting characteristics

S.A. Kulinich*, M. Farzaneh

NSERC/Hydro-Quebec/UQAC Industrial Chair on Atmospheric Icing of Power Network Equipment (CIGELE) and Canada Research Chair on Engineering of Power Network Atmospheric Icing (INGIVRE), Université du Québec à Chicoutimi, Que., Canada G7H 2B1

Received 17 January 2004; received in revised form 16 February 2004; accepted 16 February 2004

Available online 2 April 2004

Abstract

The analysis of wetting behavior of self-assembled monolayers of alkylsilanes is presented. A simple model accounting for various surface fractions of CH_3 and CH_2 groups (self-assembly order/disorder) is used. The effect of inclusion of air in the structure of rough silanized surfaces is also considered. The importance of reduced solid–water contact area and assembly order of organic monomers is demonstrated for achieving both high contact angle and low sliding angle. As coatings with low surface energy, these materials may be of potential use for ice-repellent purposes.

PACS: 68.45.G; 68.35.M

Keywords: SAMs; Low surface energy; Water contact angle; Sliding angle; Hydrophobicity; Icephobicity

1. Introduction

During cold periods, ice and snow build-up on power network equipments, such as cables, towers and insulators, sometimes causes serious problems. While efforts to develop mechanical ice removal techniques have received the most attention [1], few studies have focused on understanding the basic mechanisms of ice adhesion and the development of icephobic surfaces from the very fundamental standpoints [2–6]. Most of the recent studies indicate that there are no solid passive coatings that are able to completely prevent ice adhesion. Ideally, such a coating/material would be solid, with a long-lasting life, easy to apply, and available at a low price [1].

For ice to adhere to a surface, it is necessary for liquid water to wet the surface, i.e., to replace the existing surface–air interface with a surface–water interface. It is impossible to completely avoid surface wetting by water and to achieve a contact angle of 180° for a sessile water droplet on a surface, because the London dispersion forces would still act across any interface, and hydrophilic sites are invariably present on any practical hydrophobic surface [3]. Thus, it is not possible to produce a surface which would not be wetted by water at all and to which ice would not adhere.

The major strategies to reduce ice–surface adhesion previously proposed in the literature are: (i) to find low-energy surfaces or coatings; (ii) to introduce air between the ice and substrate; and (iii) to achieve an

* Corresponding author. Tel.: +1-418-545-5011x5053; fax: +1-418-545-5032.
E-mail address: skulinich@hotbox.ru (S.A. Kulinich).

0169-4332/$ – see front matter © 2004 Elsevier B.V. All rights reserved.
doi:10.1016/j.apsusc.2004.02.031

optimum degree of roughness, which may stimulate the formation and propagation of cracks in the ice [1,3–5].

Self-assembled organic monolayers (SAMs) on solid substrates provide an interesting approach to tailor-designed surfaces with controlled physical and chemical properties [7–12]. A class of widely used SAMs is based on *n*-alkyltrichlorosilane precursor molecules [10,13–15], which, through hydrolysis and polymerization, produce self-assembled alkylsiloxane films with low free surface energy (Fig. 1). Hydrophilic surfaces can be made hydrophobic through the self-assembly of molecules with hydrophobic "tail groups" such as *n*-alkyltrichlorosilanes. Octadecyltrichlorosilane (OTS), as the most common model compound, self-assembles into a robust monolayer on almost any high-energy surface [10,13,14]. By virtue of their hydrolysable functional groups, OTS molecules can be covalently bound to substrate hydroxyl groups, as well as cross-linked within the octadecylsiloxane layer (Fig. 1a).

In their experimental work, Somlo and Gupta have shown that ice adhesion decreases when a SAM of dimethyl-*n*-octadecilchlorosilane is formed on an Al alloy surface [6]. More recently, Petrenko and Peng have applied mixtures of self-assembling 1-dodecanethiol and 11-hydroxylundecane-1-thiol with various degrees of hydrophobicity/hydrophilicity on Au surfaces and have shown a good correlation between the contact angle of water and the ice adhesion strength [5]. However, there is still a lack of systematic knowledge on how the microstructure and surface chemistry of SAMs influence their hydrophobic and, in particular, icephobic properties.

A correlation between wettability and interfacial strength between solid surfaces and ice has been shown in a few previous studies [3–5]. As wetting, in most cases, is the first stage of an icing event, wetting behavior of hydrophobic *n*-alkylchlorosilane SAM coatings with various degrees of order/disorder is theoretically considered in this work. The analysis is done on the basis of the Israelachvili–Gee (and/or the Cassie) approach [16,17] and the Wenzel equation [18], which consider chemically heterogeneous and rough surfaces, respectively. The sliding angle is also qualitatively evaluated as a function of self-assembly order in an alkylsiloxane monolayer.

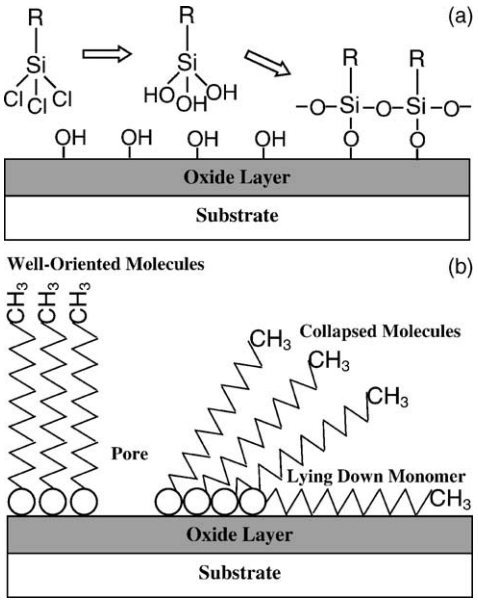

Fig. 1. Schematic representation of: (a) silanization process of alkyltrichlorosilane molecules on a substrate covered with an oxide layer and formation of an alkylsiloxane monolayer and (b) well-oriented (or close-packed) SAM molecules, pore, collapsed molecules and lying down monomers.

2. Modeling of wetting behavior

The analysis of literature shows that both continuous growth (or formation of disordered, liquid-like submonolayer species) and island-type growth (or formation of organized aggregates with vertically aligned alkyl chains) are involved in the formation of alkylsilane SAMs [10,13–15]. The relative contributions of these two mechanisms depend strongly on the experimental parameters used for film preparation [10,13–15]. In Fig. 1b, disordered species and a part of a well-organized aggregate are shown on the right and on the left, respectively. Another structural defect detected on SAMs, a pinhole or a pore with no SAM molecules adsorbed onto the surface, is also shown in Fig. 1b. It should be added that self-assembly is not the only reaction possible between alkyltrichlorosilanes and surfaces; covalent attachment and vertical polymerization of oligomers are also possible under certain conditions [19].

Taking into account the above, a model of wetting behavior for *n*-alkylsilane–SAM coatings is proposed

as follows. (i) We consider alkylsilane–SAM-grafted surfaces with surface coverage close to 1.0 (impact of pores in coatings is negligible). (ii) The distribution of the heterogeneities is assumed to be uniform over the surface, irrespective of whether they are of geometrical or chemical character. (iii) We assume that the wettability of a smooth alkylsilane-grafted surface is defined by relative contributions of methyl (CH_3) and methylene (CH_2) groups. Well-organized aggregates are terminated by methyl groups, whereas methylene groups start to be exposed as the degree of self-assembly disorder increases (Fig. 1b).

For the simplest cases of smooth and chemically inhomogeneous surfaces terminated with CH_3 and CH_2 groups, the wettability can be evaluated using the contact angle given by the Israelachvili–Gee Eq. (1) [16] and the Cassie Eq. (2) [17]. Eq. (1) is replaced by Eq. (2) when the surface is composed of well separated and distinct domains terminated by either CH_3 or CH_2 groups. The relation (1) replaces the Cassie equation whenever the size of chemically heterogeneous domains approaches molecular dimensions. Such inhomogeneity has been demonstrated, e.g., for OTS on Si and mica surfaces, when some of SAM islands formed, depending on process parameters, are smaller than 1 μm in size [10,13–15].

$$(1+\cos\theta)^2 = f_3(1+\cos\theta_3)^2 + f_2(1+\cos\theta_2)^2 \quad (1)$$

$$\cos\theta = f_3\cos\theta_3 + f_2\cos\theta_2 \quad (2)$$

where θ is the equilibrium contact angle of a chemically heterogeneous and ideally smooth surface; $\theta_3 = 110^\circ$ contact angle for pure homogeneous surfaces of CH_3 groups [8,19]; $\theta_2 = 94^\circ$ contact angle for pure surfaces of CH_2 groups [8,19,20]; and f_3 and f_2 are area fractions of methyl and methylene groups ($f_3 + f_2 = 1$), respectively.

Using Eq. (1), Almanza-Workman et al. estimated the degree of disorder of highly hydrophobic coatings deposited from water dispersible organosilanes onto pre-oxidized Si wafers. It was shown that the area fraction of methyl-terminated domains f_3 can reach 0.95 [8].

When a solid surface is rough (Fig. 2 (bottom)), Eqs. (1) and (2) are modified into the Wenzel Eq. (3)

$$\cos\theta_r = r\cos\theta \quad (3)$$

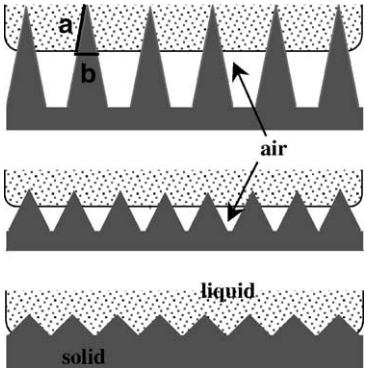

Fig. 2. Schematic representation of wetting of hydrophobic solid surfaces with various roughness. Air is entrapped beneath the water drop on the surfaces after certain increased roughness. Surface on the top is a schematic illustration of the surface model composed of a series of uniform needles which is used for the sliding-angle calculations.

where r is a roughness factor, a coefficient giving the ratio of the actual area of a rough surface to the projected area, and θ_r the contact angle on a rough surface [12,18,21,22].

Another effect of a rough hydrophobic surface with high enough value of roughness factor is air inclusion [12,23–26]. When the roughness of a solid surface increases over a certain level, the system enters a regime in which the liquid does not penetrate into the troughs (see Fig. 2) [12,23–26]. Surfaces such as these are referred to as composite surfaces, since the intersection of the water droplet with the surface consists of a composite mixture of water–solid interface area and water–air interface area. The wettability of such surfaces is described by Eq. (4)

$$\cos\theta_c = f^w\cos\theta - f^a \quad (4)$$

where θ_c is the contact angle of liquid on a rough surface with air inclusion; f^w the fraction of water–solid; and f^a the fraction of water–air interface area.

When a small amount of water is on a rough hydrophobic surface with air inclusion, the surface is only partly covered with water, Eq. (2) may be further modified into Eq. (5)

$$\cos\theta^* = f_3\cos\theta_3^* + (1-f_3)\cos\theta_2^* \quad (5)$$

where "$*$" denotes a partially air-covered surface. As will be shown below (Fig. 3), Eqs. (1) and (2) predict very close values of contact angles, therefore, for

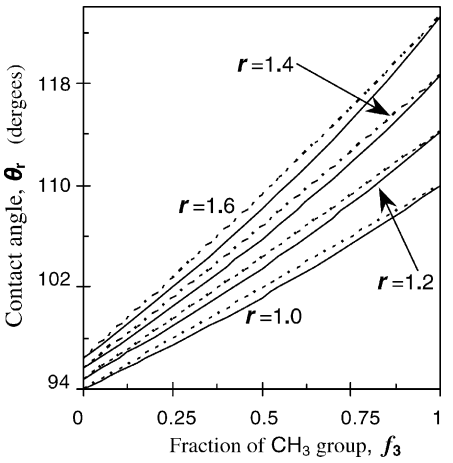

Fig. 3. Contact angle of alkylsilane–SAM-grafted surfaces as a function of the fraction f_3 of CH_3 groups exposed. For comparison, a series of curves for a smooth ($r = 1.0$) and rough surfaces ($r = 1.2$, 1.4, 1.6) are given. Results for nano- and micro-sized domains are shown by solid and dashed lines, respectively.

simplicity, Eq. (5) considers the chemically non-homogeneous surface with micro-sized domains. Then, the surfaces of both CH_3- and CH_2-terminated domains may be divided into two parts, one being covered with water and the other with air with the area ratios $f_3^w : f_3^a$ and $f_2^w : f_2^a$, respectively. Here, $f_i^w + f_i^a = 1$ $(i = 2, 3)$ and superscripts "w" and "a" denote water and air, respectively. Thus, taking Eq. (4) into consideration, $\cos\theta_3^*$ and $\cos\theta_2^*$ may be expressed as follows:

$$\cos\theta_3^* = f_3^w \cos\theta_3 + f_3^a \cos 180^\circ = f_3^w(1 + \cos\theta_3) - 1 \quad (6)$$

and

$$\cos\theta_2^* = f_2^w \cos\theta_2 + f_2^a \cos 180^\circ = f_2^w(1 + \cos\theta_2) - 1 \quad (7)$$

Combining Eqs. (5)–(7) leads to Eq. (8), which can be used to evaluate the equilibrium contact angle on rough chemically inhomogeneous surfaces with air pockets

$$\cos\theta^* = f_3(f_3^w(1 + \cos\theta_3) - 1) + (1 - f_3)(f_2^w(1 + \cos\theta_2) - 1) \quad (8)$$

In a few recent studies, it has been proposed that the static contact angle itself is not sufficient to completely characterize a water-repellent surface; dynamic wettability, which is described by means of the sliding angle of a water droplet, is also very important and should be taken into account [23–26]. To evaluate the sliding angle of rough SAM-grafted surfaces as a function of the CH_3 fraction f_3 (order/disorder degree of self-assembly), Eq. (9) is used. Eq. (9) was proposed by Miwa et al. [26] to describe sliding angles of water droplets on rough surfaces, which are composed of a series of uniform needles, as illustrated in Fig. 2 (top).

$$\sin\alpha = \frac{2Rk\sin\theta^*(\cos\theta^* + 1)}{g(R\cos\theta + 1)} \times \sqrt[3]{\frac{3\pi^2}{m^2\rho(2 - 3\cos\theta^* + \cos^3\theta^*}} \quad (9)$$

where α is the minimum angle of surface tilt at which a droplet will spontaneously move; R the ratio of the side area to the bottom area of the needle, which is defined by the ratio a/b in Fig. 2 (top); θ and θ^* are contact angles on flat and rough surfaces (determined from Eqs. (2) and (8)), respectively; m and ρ the mass and specific weight of the liquid droplet, respectively; g is the gravitational acceleration; and k a constant with a dimension of mJ/m^2, which was related by Murase and Fujibayashi to the interaction energy between solid and liquid [27].

3. Results and discussion

3.1. Effect of assembly order/disorder and surface roughness

Fig. 3 shows the influence of the degree of alkylsilane molecule self-assembly on the contact angle of a sessile water droplet, as calculated from Eqs. (1) and (2). As expected from Eqs. (1) and (2), for the same values of θ_3, θ_2, f_3, and f_2, the Cassie equation always predicts somewhat greater contact angles than those obtained from Eq. (1) (dashed and solid lines in Fig. 3). It should also be noted that when we go from molecular-sized domains (solid lines) to larger domains (dashed lines), there should also be a progressive increase in the contact angle hysteresis [16]. The latter may play an important role in determining the sliding angle of a water droplet on a tilted surface. The constant increase of the contact angle as a function of f_3 (degree of self-assembling order) is observed,

implying the importance of controlling this factor when SAMs with improved water repellency are to be produced.

It can also be observed in Fig. 3 that the water contact angle of rough SAM-grafted surfaces, calculated using Eq. (3) for $r = 1.2$, 1.4, and 1.6, increases constantly when compared to that on a flat surface (curves marked with $r = 1.0$). Thus, rougher substrates allow increasing static contact angle of water droplets. It should be mentioned that surface roughness of hydrophobic SAM-coated materials can be controlled, e.g., by depositing a SiO_2 (or Al_2O_3) underlayer with a desirable surface morphology [11], by means of substrate patterning [12,28], by sol–gel technique [23], or by plasma etching of the substrate before the SAM film is formed [29].

3.2. Effect of air inclusion

The previous work has demonstrated that the air trapped in the surface structure plays an important role for a surface with a high hydrophobicity and/or low sliding angle [12,22–26]. Fig. 4 presents the relation between θ^*, as calculated from Eq. (8), and f_3 and f_3^w. Three different cases of water coverage of methylene-terminated domains with $f_2^w = 0.2$ (a), 0.5 (b), and 0.8 (c) are shown. It is clearly seen that the highest values of θ^* are attained when f_3^w and f_2^w are lower (more air trapped in surface structure) and CH_3 fraction f_3 is increased (higher assembly order of SAM molecules). When water coverage of methylene-terminated domains is increased (in Fig. 4(a–c), $f_2^w = 0.2$, 0.5, and 0.8, respectively), the contact angle θ^* decreases,

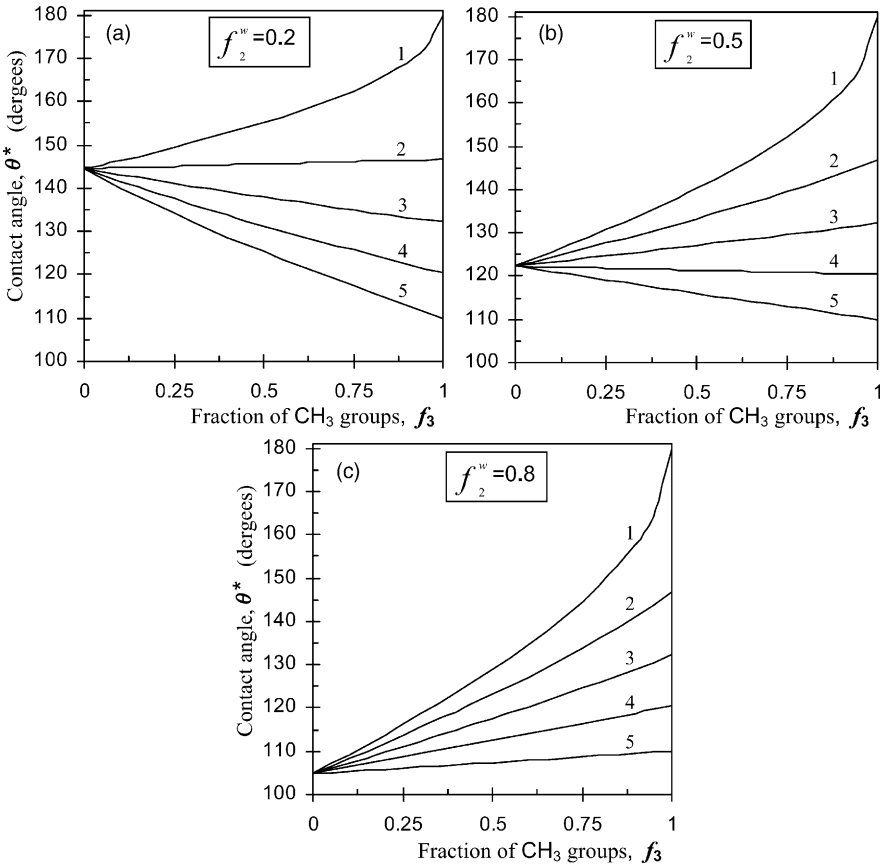

Fig. 4. Contact angle of alkylsilane–SAM-grafted surfaces as a function of the fraction f_3 of CH_3 groups in a composite-surface wetting regime with air entrapped. The cases of surface coverage of methylene-terminated phase with water equal to: (a) $f_2^w = 0.2$; (b) $f_2^w = 0.5$; and (c) $f_2^w = 0.8$ are presented. Curves for water coverage of methyl-terminated phase $f_3^w = 0$, 0.25, 0.5, 0.75, and 1 are marked as 1, 2, 3, 4, and 5, respectively.

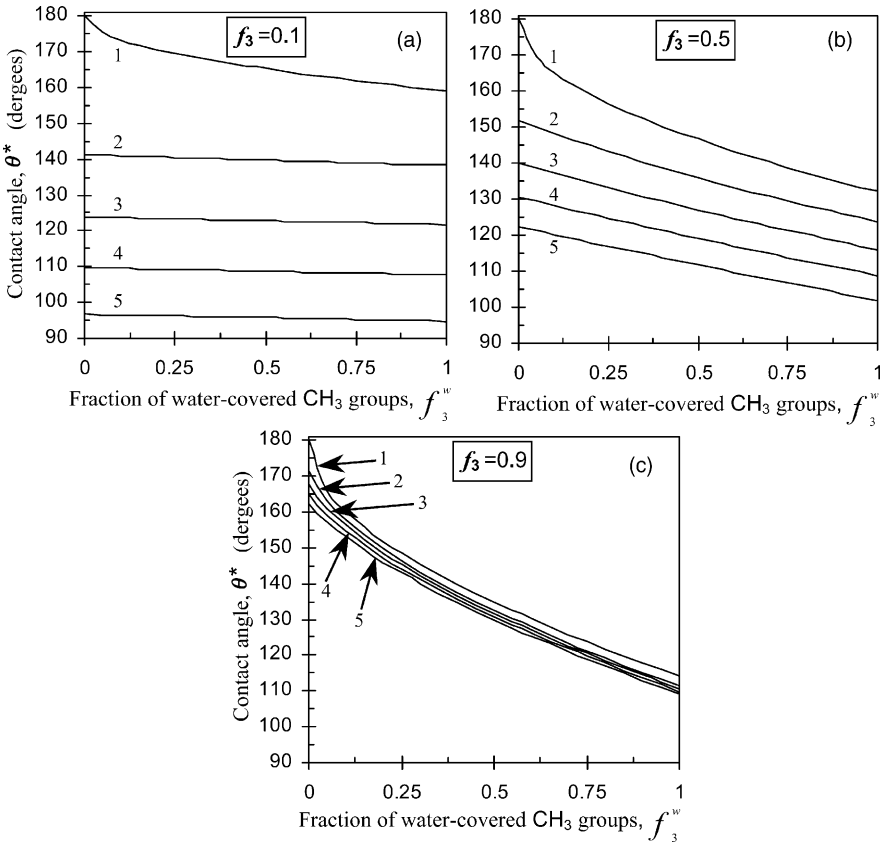

Fig. 5. Contact angle of alkylsilane–SAM-grafted surfaces as a function of the fraction f_3^w of water-covered CH_3 groups in a composite-surface wetting regime with air entrapped. The cases of surface coverage with methyl-terminated phase, f_3, equal to: 0.1 (a); 0.5 (b); and 0.9 (c) are presented. Curves for water coverage of methylene-terminated phase $f_2^w = 0$, 0.25, 0.5, 0.75, and 1 are marked as 1, 2, 3, 4, and 5, respectively.

however, its tendency, with respect to f_3 and f_3^w, remains the same as for low values of f_2^w. It should be added that situations when $f_2^w \leq f_3^w$ are hardly expected in wetting of real heterogeneous surfaces, since CH_2-terminated domains are less hydrophobic compared to CH_3-terminated ones [30]. And therefore, materials described by the curves 2–5 in Fig. 4a; curves 4 and 5 in Fig. 4b; and curve 5 in Fig. 4c cannot be obtained in practice.

The same tendencies are also demonstrated in Fig. 5, where the relation between θ^* and f_3^w and f_2^w, also obtained from Eq. (8), is given for three $f_3 = 0.1$ (a), 0.5 (b), and 0.9 (c). Again, larger fraction f_3 and lower water coverage of methyl-terminated (f_3^w) and methylene-terminated (f_2^w) domains lead to higher values of apparent contact angle θ^* on a rough alkylsilane-coated surface with air inclusions. As expected, the influence of water coverage of CH_2-terminated domains is the strongest at low fraction of methyl-terminated domains f_3 (Fig. 5a), whereas it becomes negligible when the surface SAM assembly order is improved ($f_3 = 0.9$ in Fig. 5c). It is also shown in Figs. 4 and 5 that contact angles of water of much more than 110° (which is the maximum possible for a smooth SAM-grafted surface with $f_3 = 1$) can be achieved on rough surfaces with air inclusion.

3.3. Sliding angle

It is commonly accepted that in the case of heterogeneous surfaces, it is domains with lower contact angle that are preferably wetted rather than those with

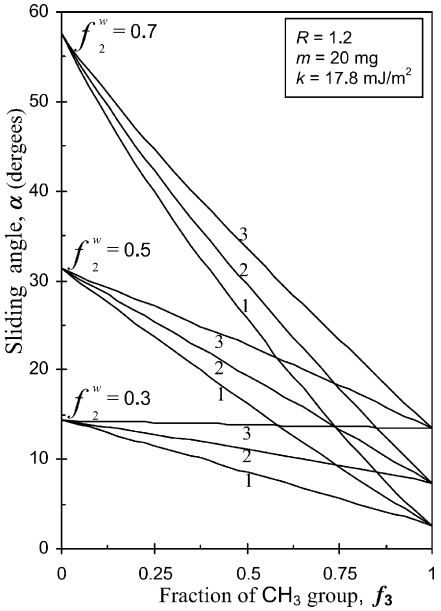

Fig. 6. Sliding angle of alkylsilane–SAM-grafted surfaces as a function of the fraction f_3 of CH_3 groups in a composite-surface wetting regime with air entrapped. Three series of curves for $f_2^w = 0.3$, 0.5, and 0.7 are given; curves for $f_3^w = 0.1$, 0.2, and 0.3 are marked as 1, 2, and 3, respectively. Results were obtained for the surfaces with $R = 1.2$ and $k = 17.8\ \mathrm{mJ/m^2}$ and for a water droplet with $m = 20$ mg.

higher contact angle [30]. Since $\theta_3 > \theta_2$, in Fig. 6 only sliding angles for a few differently wetted SAM-grafted surfaces with $f_3^w \leq f_2^w$ are shown. The results were obtained from Eq. (9) in combination with Eqs. (2) and (8). Thus, as in the previous section, rough alkylsilane-grafted surfaces with air pockets and micro-sized CH_3- and CH_2-terminated domains are considered.

Fig. 6 shows three sets of sliding-angle curves for alkylsilane–SAM surfaces, where diverse regimes of water coverage of methylene-terminated domains are realized, i.e., $f_2^w = 0.3$, 0.5, and 0.7, respectively. For each f_2^w, three curves for various water coverage of methyl-terminated domains $f_3^w = 0.1$, 0.2, and 0.3 (marked as 1, 2, and 3, respectively) are presented. The calculations were made for surfaces with $R = 1.2$ in accordance with the surface model of Miwa et al. [26], shown in Fig. 2 (top), and for a water droplet with $m = 20$ mg. For simplicity, the constant k was chosen to be equal to 17.8 mJ/m^2 and independent of SAMs' order/disorder degree. This value was reported by Wolfram and Faust as the experimental constant for the smooth water–polypropylene system [31]. We chose this datum as polypropylene surface is also composed of CH_2 and CH_3 groups. The surfaces represented in Fig. 6 by sliding-angle curves, demonstrate the water contact angles of 113–138° at $f_3 = 0.1$, 125–146° at $f_3 = 0.5$, and 139–156° at $f_3 = 0.9$ (from Eq. (8) and Fig. 5). Thus, sliding behavior is presented for hydrophobic or highly hydrophobic SAM-grafted surfaces.

It is apparent from Fig. 6 that low water sliding angles may be attained on highly hydrophobic surfaces which are designed with the lowest possible water-coverage fractions of both CH_3- and CH_2-terminated domains, f_3^w and f_2^w. Because of higher air ratio at the solid–water interface, their sliding resistance is reduced, and lower sliding angles are attained in this model. It is also seen that increasing f_3 reduces water sliding angles, thus improving both static (see previous sections) and dynamic hydrophobicity. Note that since ice and wet-snow accumulations, in many cases, come from supercooled water droplets and ice particles, materials with low sliding angles may be very attractive as ice- and snow-repellent ones, because water droplets are not easily pinned on their surfaces.

Strictly speaking, the constant k, as being related to the interaction energy between solid and liquid [26,31], should depend on f_3 (i.e., surface energy of solid). In general, k should be larger for very low values of f_3 and lower for high f_3, which is expected to result in even greater sliding angles at low f_3 and lower ones at high f_3 (see Eq. (9)). Thus, Fig. 6 shows only a qualitative idea of sliding angle behavior for the hydrophobic surfaces under consideration.

It should also be mentioned that the curves drawn in Figs. 4 and 6 present surfaces with same wetting parameters (constant f_3^w and f_2^w for each curve) rather than with same geometrical topologies. The assumption of constant R should not necessarily be satisfied for surfaces with same topologies but coated with differently assembled SAMs. When f_3 increases from 0 to 1, R is expected to slightly decrease, since coated with more hydrophobic topmost CH_3 groups surface needles (Fig. 2, top) may tend to hold water only on the extreme top portions. According to Ref. [26], R may approach 1 for surfaces with very high water contact angles. Thus, when f_3 increases for surfaces

with same geometrical topographies, both f_3^w and f_2^w parameters are expected to slightly decrease, and thus, both wetting and sliding behavior of the surfaces should be described by corresponding curves with lower values of f_3^w and f_2^w (see Figs. 4 and 6).

3.4. Critical notes

Based on the results obtained, the following ways to enhance water repellency, and probably icephobicity, of alkylsilane–SAM-grafted surfaces are proposed:

(i) Use of fluoroalkylsilane–SAMs with CF_3 and CF_2 groups in alkyl chain [12,23,29,32–34]. This should result in additional decrease in free surface energy and, consequently, water–solid interface interaction.
(ii) Use of rough substrates [11,12,23,29]. As was shown, higher contact angles and reduced sliding angles can be attained with rough surfaces with air inclusion.
(iii) Use of specially designed/patterned surfaces to improve air inclusion [12,23–25,35,36]. The topological nature of the surface roughness is important in determining hydrophobicity; a proper interval and height difference in the microstructure are of prime importance to provide both high contact angles and low sliding angles for rough hydrophobic surfaces [24,25,35]. According to the recent approach of Öner and McCarthy [24,25], to decrease water sliding angles, a properly designed surface is expected to not allow continuous contact of a liquid with the surface and to demonstrate little or no difference in energy between different metastable states. As a result, the liquid droplet would not remain pinned in metastable state and would move spontaneously on such a surface.
(iv) Formation of SAMs with the highest possible assembly degree [8,10,13–15]. As was shown, this increases water contact angles and reduces sliding angles, thus improving both static and dynamic water repellency. While in the literature this parameter is often ignored [6,26,29], one of the main objectives of this work was to stress out the importance of control of the assembly degree of SAM coatings, when the surface hydrophobicity (and probably icephobicity) is concerned.

It has been shown by Saito et al. that the ice adhesion to the rough polytetrafluoroethylene coatings decreases with increasing water contact angles [37], thus implying a direct relationship between hydrophobicity and icephobicity for certain rough materials with low surface energy. As it is known, rough hydrophilic surfaces allow deep water penetration into the surface, thus resulting in the anchor effect and larger ice adhesion. In contrast, when a water-repellent surface becomes rougher, air pockets are formed (see Fig. 2, top) [12,22,24–26]. As a result, the anchor effect and adhesion strength between ice and such a material can be much reduced. From this point of view, properly designed/patterned rough SAM-grafted surfaces with well-assembled alkylsilane molecules are expected to be good candidates as icephobic materials.

It should, however, be added that the approach used in this study does not account for the geometry/topography of the surface under consideration. So far, there has been only limited research on how surface shapes and dimensions (rough topology) govern static and/or dynamic hydrophobicity of rough surfaces [12,24–26]. Thus, additional work, combining both experimental and theoretical approaches, is needed to further understand the wetting behavior of SAM-coated surfaces with high roughness.

4. Conclusion

Wetting characteristics of alkylsilane self-assembling monolayer coatings, as potential snow- and ice-repellent materials with low and controllable surface energy, are theoretically investigated in a wide range of both self-assembly degree and surface roughness. The analysis is based on the Wenzel equation, which takes into account surface roughness, and the Cassie or Israelachvili–Gee equations that consider chemically inhomogeneous surfaces. It is shown that both static (determined by the contact angle) and dynamic water repellency (determined by the sliding angle) of an alkylsilane-grafted surface are strongly influenced by the degree of self-assembly of alkylsilane molecules and by water coverage of a rough surface, which can trap air. Highly ordered coatings of alkylsilane molecules and reduced solid–water contact area, caused by a substrate roughness, lead to considerably

enhanced hydrophobicity of the surface. Further systematic work, involving both experimental and theoretical approaches, is needed to develop alkylsilane–SAM coatings with improved water- and ice-repellent properties.

Acknowledgements

This research was carried out within the framework of the NSERC/Hydro-Quebec/UQAC Industrial Chair on Atmospheric Icing of Power Network Equipment (CIGELE) and Canada Research Chair on Engineering of Power Network Atmospheric Icing (INGIVRE) at Université du Québec à Chicoutimi. The authors would like to thank all the partners of CIGELE/INGIVRE for their financial support. They would also like to thank Dr. M.R. Kasaai for useful discussions.

References

[1] J.L. Laforte, M.A. Allaire, J. Laflamme, Atmos. Res. 46 (1998) 143–158.
[2] H.H.G. Jellinek, Can. J. Phys. 40 (1962) 1294–1309.
[3] V.K. Croutch, R.A. Hartley, J. Coat. Technol. 64 (1992) 41–52.
[4] L.O. Andersson, C.G. Golander, S. Persson, J. Adhes. Sci. Technol. 8 (1994) 117–132.
[5] V.F. Petrenko, S. Peng, Can. J. Phys. 81 (2003) 387–393.
[6] B. Somlo, V. Gupta, Mech. Mater. 33 (2001) 471–480.
[7] A. Ulman, Chem. Rev. 96 (1996) 1533–1554.
[8] A.M. Almanza-Workman, S. Raghavan, S. Petrovic, B. Gogoi, P. Deymier, D.J. Monk, R. Roop, Thin Solid Films 423 (2003) 77–87.
[9] M. Aslam, N.K. Chaki, J. Sharma, K. Vijayamohanan, Curr. Appl. Phys. 3 (2003) 115–127.
[10] C. Carraro, O.W. Yauw, M.M. Sung, R. Maboudian, J. Phys. Chem. B 102 (1998) 4441–4445.
[11] Y. Wu, H. Sugimura, Y. Inoue, O. Takai, Thin Solid Films 435 (2003) 161–164.
[12] Z. Yoshimitsu, A. Nakajima, T. Watanabe, K. Hashimoto, Langmuir 18 (2002) 5818–5822.
[13] D.K. Schwartz, S. Steinberg, J. Israelachvili, J.A.N. Zasadzinski, Phys. Rev. Lett. 69 (1992) 3354–3357.
[14] D.W. Britt, V. Hlady, J. Colloid Interface Sci. 178 (1996) 775–784.
[15] T. Vallant, H. Brunner, U. Mayer, H. Hoffmann, T. Leitner, R. Resch, G. Friedbacher, J. Phys. Chem. B 102 (1998) 7190–7197.
[16] J.N. Israelachvili, M.L. Gee, Langmuir 5 (1989) 288–289.
[17] A.B.D. Cassie, Discuss. Faraday Soc. 3 (1948) 11–16.
[18] R.N. Wenzel, Ind. Eng. Chem. 28 (1936) 988–994.
[19] A.Y. Fadeev, T.J. McCarthy, Langmuir 16 (2000) 7268–7274.
[20] E.L. Decker, S. Garoff, Langmuir 13 (1997) 6321–6332.
[21] D. Quéré, Physica A 313 (2002) 32–46.
[22] A. Nakajima, K. Hashimoto, T. Watanabe, Monatsh. Chem. 132 (2001) 31–41.
[23] A. Nakajima, K. Abe, K. Hashimoto, T. Watanabe, Thin Solid Films 376 (2000) 140–143.
[24] W. Chen, A.Y. Fadeev, M.C. Hsieh, D. Öner, J. Youngblood, T.J. McCarthy, Langmuir 15 (1999) 3395–3399.
[25] D. Öner, T.J. McCarthy, Langmuir 16 (2000) 7777–7782.
[26] M. Miwa, A. Nakajima, A. Fujishima, K. Hashimoto, T. Watanabe, Langmuir 16 (2000) 5754–5760.
[27] H. Murase, T. Fujibayashi, Prog. Org. Coat. 31 (1997) 97–104.
[28] Y. Xia, D. Qin, Y. Yin, Curr. Opin. Colloid Interface Sci. 6 (2001) 54–64.
[29] K. Ogawa, M. Soga, Y. Takada, I. Nakayama, Jpn. J. Appl. Phys. 32 (1993) L614–L615.
[30] P. Lenz, Adv. Mater. 11 (1999) 1531–1534.
[31] E. Wolfram, R. Faust, Liquid drops on a tilted plate, contact angle hysteresis and the Young contact angle, in: J.F. Padday (Ed.), Wetting, Spreading and Adhesion, Academic Press, London, 1978, pp. 213–222.
[32] H.-J. Jeong, D.-K. Kim, S.-B. Lee, S.-H. Kwon, K. Kadono, J. Colloid Interface Sci. 235 (2001) 130–134.
[33] A. Nakajima, A. Fujishima, K. Hashimoto, T. Watanabe, Adv. Mater. 11 (1999) 1365–1368.
[34] A. Nakajima, K. Hashimoto, T. Watanabe, K. Takai, G. Yamauchi, A. Fujishima, Langmuir 16 (2000) 7044–7047.
[35] H. Nakae, R. Inui, Y. Hirata, H. Saito, Acta Mater. 46 (1998) 2313–2318.
[36] J.-G. Fan, X.-J. Tang, Y.-P. Zhao, Nanotechnology 15 (2004) 501–504.
[37] H. Saito, K. Takai, G. Yamauchi, Surf. Coat. Int. 80 (1997) 168–172.